Trans Indian Inst Met (2021) 74(7):1721–1728
https://doi.org/10.1007/s12666-021-02267-w

ORIGINAL ARTICLE

Effects of Cr Microalloying on Structural Evolution, Crystallization Behavior and Micromechanical Properties of ZrCoAlCr Bulk Metallic Glass

Supriyono[1] · A. Surendar[2] · Lakshmi Thangavelu[3] · Zeinab Arzehgar[4] · Michail V. Pokrovskii[5] · Dmitriy A. Neganov[6] · Dmitrii K. Goncharov[7] · Harsha Mohanty[8]

Received: 3 November 2020 / Accepted: 18 April 2021 / Published online: 9 May 2021

Abstract This paper deals with the role of minor addition of Cr on the atomic rearrangement and crystallization evolution in a Zr-based bulk metallic glass. For this purpose, Cr elements with 1–4% atomic percentage were added into the alloying composition. The X-ray diffraction results indicated that the trace element led to the increase in disordered structures in the glassy alloy and the decline in population of short and medium scale orders. This event was due to the intensification of structural heterogeneity which was manifested in the change of enthalpy relaxation. The differential scanning calorimetry analysis also showed that all ZrCoAlCr BMG samples included two distinct crystallization peaks during the heating process. However, the increase in Cr content led to the intensification of low temperature peak. This result was consistent with viscosity analysis, in which the viscosity decrement was intensified at the range of low temperature crystallization peak with the rise in Cr content. Moreover, it was found that although the plasticity improved in samples with Cr-content, the strength showed a slight decrease.

Keywords Crystallization · Atomic structure · Microalloying · Bulk metallic glass

✉ Harsha Mohanty
mohanty.har1985@gmail.com

[1] Department of Mechanical Engineering, Faculty of Engineering, Universitas Muhammadiyah Surakarta, Surakarta, Indonesia

[2] Department of Pharmacology, Saveetha Dental College and Hospital, Saveetha Institute of Medical and Technical Sciences, Chennai, India

[3] Department of Pharmacology, Saveetha Dental College and Hospital, Saveetha Institute of Medical and Technical Sciences, Saveetha University, Chennai, India

[4] Department of Chemistry, Payame Noor University, 19395-4697 Tehran, Iran

[5] Belgorod State University, Belgorod, Russia

[6] Kazan Federal University, Kazan, Russia

[7] Department of Informatics, Plekhanov Russian University of Economics, Moscow, Russia

[8] Department of Mining Engineering, National Institute of Technology Karnataka, Surathkal, Mangaluru, India

1 Introduction

Owing to their unique structural features and outstanding functional and mechanical properties, bulk metallic glasses (BMGs) are known as promising materials for a wide range of applications [1–5]. However, it is hard to fabricate them with thickness in centimeters, which is due to their glass forming ability (GFA) [6]. Moreover, the limited plasticity under external loadings is a big challenge for applying them in many engineered structures [7–9]. This phenomenon is a result of the mechanism of localized deformation, which is manifested by the appearance of shear bands. Several approaches have been proposed to tackle these problems [10–13]. Among them, minor addition of elements, i.e., microalloying process, is one of the main techniques being able to simultaneously affect the GFA and plasticity in the BMGs [14–17]. The option of element type is closely associated to the chemical compositions of BMG and certain mechanism for the GFA improvement [18]. As an illustrated, Zai et al. [19] added Ga element into the MgZnCa system and found that the 1 at.% Ga microalloying led to the significant improvement of casting critical diameter and fracture strength. Bera et al. [20] revealed that Ga element also enhanced the plasticity

properties of TiZrCuPd amorphous system by inducing local structural heterogeneity in the atomic configuration of BMG. In another study, it is reported that the Ni microalloying provide significant constraint on the crystallization initiation of a Cu-based BMG [21]. Samavatian et al. [22] showed that the Nb minor addition with positive heat of mixing (Zr–Nb) in ZrCuNiAl led to the increase in population of short- and medium-range orders and tighten the atomic arrangement. Using Hf element in a ZrTiCuAl BMG, it was found out that minor addition remarkably enlarged the super-cooled liquid region and reached the critical diameter from 4 to 8 mm [23]. Cai et al. [24] investigated the role of Al microalloying on the properties of CuZrTi BMG and related that glass transition activation energy enhanced in an optimum minor addition. Adding rare-earth metal Er, Malekan et al. [25] recognized that the surprising GFA of 15 mm in diameter for Cu–Zr–Al BMGs, was due to the quaternary composition with a deep eutectic. Heavy rare-earth metals were also studied by other researchers and it was found that the rare-earth-element microalloying led to severe change of atomic configurations and electronic structures [26]. Employing molecular dynamic simulation, it was discovered that minor addition of Y increased the icosahedra and Kasper polyhedra with high local five-fold symmetry in a MgCuY amorphous system and improved the GFA properties [27]. Mizuno et al. [28] revealed that the minor addition of oxygen, even in ppm, led to the significant changes in the critical cooling rate of the glassy alloys.

According to literature [22, 23, 28], microalloying from metalloid elements to rare-earth ones may lead to the improvement of GFA and mechanical behaviors in the BMGs. However, the mechanisms for betterment of properties are still under debate. For example, the minor addition of elements would result in degradation of the GFA. On the other side, proper addition may tighten the alloy structure [29]. To better understand the microalloying mechanism, this work aims to show that how negative heat of mixing for Cr element can change the inherent features of glasses. For this purpose, Cr was added into a Zr-based BMG with a two potential crystalline phases to elaborate the microalloying effects on the glassy systems.

2 Materials and Methods

Under an argon environment, the Zr, Al, Co and Cr metals with 99.99% high purity were prepared and alloyed in the form of ingots using arc remelting technique. The nominal composition of base alloy was $Zr_{60-x}Co_{25}Al_{15}Cr_x$ (x = 0, 1, 2, 3, 4). To prepare glassy rods with 2 mm diameter, the ingots were then fabricated by suction casting process in a water-cooled copper mold. In BMG alloys, the purity of melt plays a significant role on the final properties of material. Hence, it is very important to consider a procedure leading to a clean casting process. To achieve this goal, the casting chamber was equipped with the rotary vacuum and diffusion vacuum pumps providing an atmosphere with the pressure of 4×10^{-5} torr. Moreover, argon gas with a high purity of 99.9999% was used for the arc melting process. This procedure led to the production of the BMG samples with no contaminating elements such as O, N and C.

After sample preparation, the X-ray diffraction (XRD) analysis was done to evaluate the amorphousness and atomic structure of BMGs. The differential scanning calorimetry (DSC) was performed under argon atmosphere and heating rate of 20 K/min to study the thermal features. For investigating the viscosity parameter, thermal mechanical analyzer (TMA) under the vacuum of 2×10^{-3} torr and a certain temperature range was carried out. The heating rate and constant load were 3 K/min and 4 N, respectively. Nanoindentation was also performed to measure the micromechanical properties of BMGs with different chemical compositions. The process was done up to maximum load of 30 mN with the loading rate 20 mN/min. The holding time of 4 S was also considered for the test. Five indenting test was done for each sample to ensure the reliability of data acquisition.

3 Results and Discussion

Fabrication of ZrCoAl-based BMGs with minor addition of elements is a good choice for having glassy alloys with good GFA and excellent mechanical properties [30–34]. The Cr atom has a negative heat of mixing with other constituents and is able to form high strength bonds in the atomic configuration of our BMG. Hence, it is possible to produce ZrCoAlCr BMGs with superior physical and mechanical behaviors. Figure 1a shows the XRD patterns for the fabricated BMG specimens. Based on the results, there are no sharp peak intensities in the curves and a broad diffused diffraction peak along with a distinctive shoulder at its right side is detected, which indicates the amorphous structure of samples. Moreover, a slight decrease in the broad peak angle and shoulder position is detected with the increase in Cr content; however, the shoulder angle again increases at the 4% Cr content. Using Bragg law and following equations, it is possible to QUALITAVELY evaluate the structure of glassy alloys [20]. Bragg law equation is established for peak intensities in crystalline materials as follow:

$$2d \cdot \sin\theta = \lambda \quad (1)$$

Considering the equation, the diffraction angle is

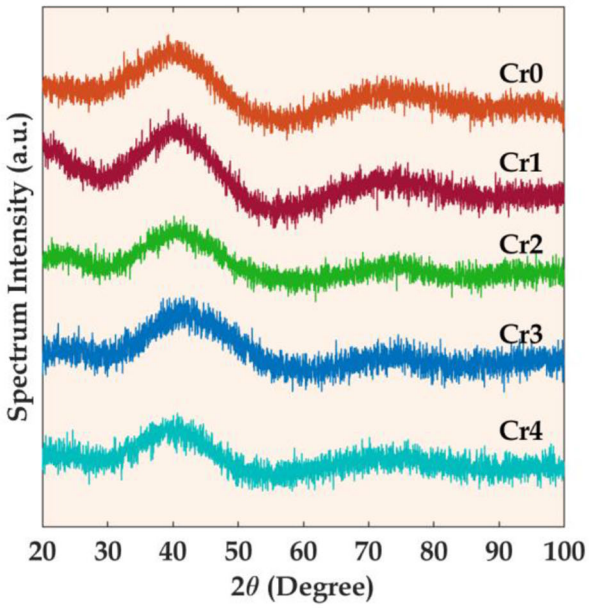

(a)

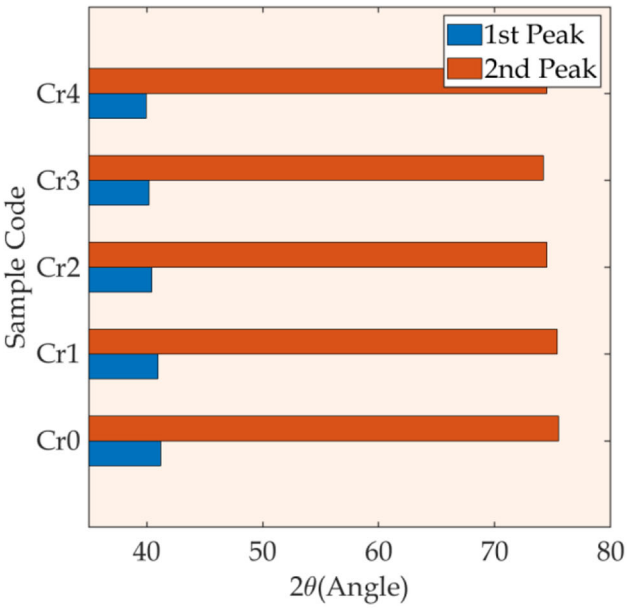

(b)

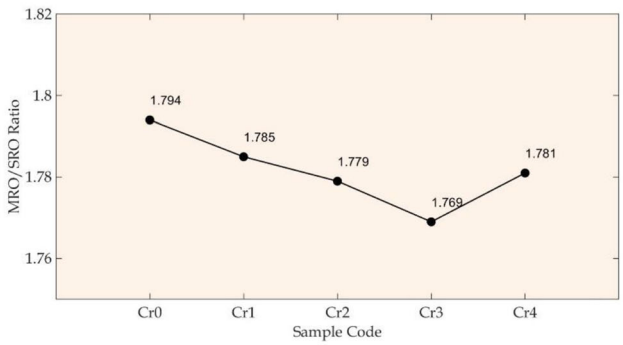

(c)

Fig. 1 **a** XRD patterns for the BMG specimens. **b** 2θ for the first diffuse peak and the second peak (top site of shoulder). For accurate detection of first peak position and top site of shoulder, Gaussian fitting with tiny errors was carried out. **c** MRO/SRO ratio, which is defined based on the ratio of peak and shoulder positions

reversely correlated to the inter-planar distance (d). On the other side, amorphous alloys lack the long range orders (LROs). Hence, the Bragg law pales into insignificance and Ehrenfest equation with consideration of broad diffraction maxima and the mean interatomic distance comes into play [20]:

$$Q = 1.23\frac{2\pi}{r} \tag{2}$$

In which r is the mean interatomic distance and Q defines the wave factor and is related to the diffraction angle [20]:

$$Q = \frac{4\pi \cdot \sin\theta}{\lambda} \tag{3}$$

Hence, the diffraction angle can be introduced as:

$$\sin\theta = \frac{1.23\lambda}{2r} \tag{4}$$

According to Eq. 4, the decrease in diffraction angle lead to the rise in mean interatomic distances. It is believed that the increase in the number of atom types in the structure leads to the enhancement of disordering events and the decrease in population of short range orders (SROs) [35, 36]. Hence, one can see that the interatomic distances slightly increase in the atomic configuration of BMG. It is also observed that the rate of decrease in diffraction angle is reduced with the increase in Cr content (see Fig. 1b). This event indicates that the disordering structure, such as free volume, may be saturated in the material. The maxima positions in the shoulders can also be evaluated with the mentioned equations. This part of XRD patterns is closely correlated to the atomic rearrangements, especially at the medium-range order (MRO) [20]. Considering this fact, one can see that the Cr addition firstly lead to the annihilation of MRO structures; however, the 3% Cr is an outset for the reconstruction of medium-range rearrangements in the atomic configuration of glass. To better understand the features of SRO and MRO configurations in the BMG, the positional ratio of diffraction and shoulder peaks was calculated and considered as the MRO/SRO ratio. As given in Fig. 1c, the MRO/SRO ratio gradually and continuously decreases up to 3% and then a slight rise appears at sample Cr4. Considering this result (see Fig. 1b,c), one can conclude that the Cr addition leads to the decline of SRO and MRO structures in the material. As clear in Fig. 1c, the decreasing trend up to 3% Cr shows that the rate of MRO annihilation is more than SRO destructions. However, for the samples with 4% Cr, a slight increase in MRO structures is seen. This shows that the excessive addition of Cr may lead to the strengthening in connection with nanoscale clusters in the BMG.

Figure 2 illustrates the DSC curves of samples in a specific range of temperature. Two sharp exothermic peaks in the curves indicate that the crystallization in the Zr-based BMG includes two distinctive phase formation. The glass transition event is also located at the lower temperature range in the vicinity of first crystallization peak. For the Cr-free sample, the first peak is much smaller than the high temperature peak. With minor addition of Cr into the composition, the first peak intensifies so that it become bigger than the second one after microalloying of 3% Cr. However, the first crystallization peak experiences a slight reduction at 4% Cr content. This result is consistent with the fact that the Cr addition may lead to the changes in the potential landscape of crystallization in the system. In other words, when the trace element is added up to 3%, the SRO and MRO structures tend to be annihilated. This phenomenon is accompanied with the increase in the free volumes and the intensification in structural heterogeneity [37–39]. As a result, the diversity of energy levels rises in the material and consequently the conditions for crystallization change, in comparison with the Cr-free BMG. In our case, one can see that the Cr atoms induce the low temperature crystallization in the structure, which means that the added atoms alter the microstructure somehow to reduce the energy barrier for the low temperature crystallization. On the other side, at 4% Cr content, the MRO arrangements again increase in the atomic configuration

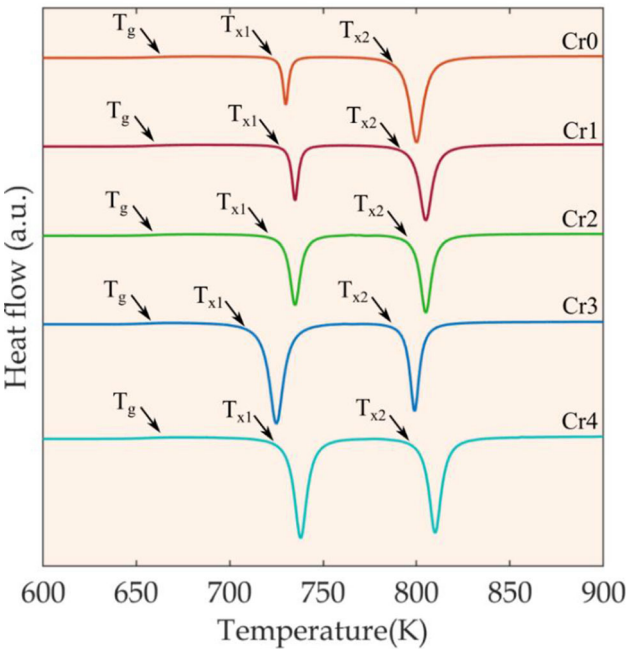

Fig. 2 Thermal curves of samples showing the crystallization peaks

and consequently a balance between two peaks appear. Our results also confirm that the MRO structure is much important than the SRO ones for changing the crystallization evolution. With minor addition of Cr from 1 to 4%, the SRO arrangement continuously decreases, while the MRO structure shows a reverse trend after 3% Cr addition. Hence, it is derived that the MRO arrangements are more efficient in the change of local energy levels in the BMGs.

Figure 3 represents the relaxation zone of BMG samples taken from the DSC curves. Based on the results, the enthalpy of structural relaxation increases with the minor addition of Cr into the alloying system; however, it is evident that the increasing trend becomes slow at the end. This outcome is well consistent with our XRD results, which show that the structural ordering declines with Cr addition, and therefore, the enthalpy relaxation rises in the material. As observed in Fig. 1b, c, the SRO structure shows a decreasing trend with rise in Cr content; however, the MRO configuration has a slight rise in sample Cr4 (4% Cr content) after showing a decreasing trend from 0 to 3% Cr content. Moreover, Fig. 3 confirms that the enthalpy relaxation continuously enhances with the Cr increment. From these results, it is reasonable to conclude that the disordering event, i.e., annihilation of SRO and MRO structures, from 0 up to 3% Cr content is accompanied with the increase in enthalpy relaxation as reported in numerous works [22, 40]. On the other side, it is also observed that the increase in enthalpy relaxation likewise is seen in sample with 4% Cr content, in which the MRO structure shows a slight enhancement (see Fig. 1c). Consequently, a competition between the SRO reduction and MRO enhancement in the 4% Cr sample is observed, which leads to very slight increase in the enthalpy relaxation. Here, it is worth mentioning that it is possible to decrease the number of SRO clusters and increase the MRO arrangements simultaneously. There are a huge number of SRO clusters with isolated features [41, 42]. Although it is possible to annihilate the isolated SRO clusters with various kind of treatments, the MRO arrangements can be intensified by connecting the remaining SRO ones [43]. Hence, the contradictory behavior of SRO and MRO arrangements can be usual in the BMGs.

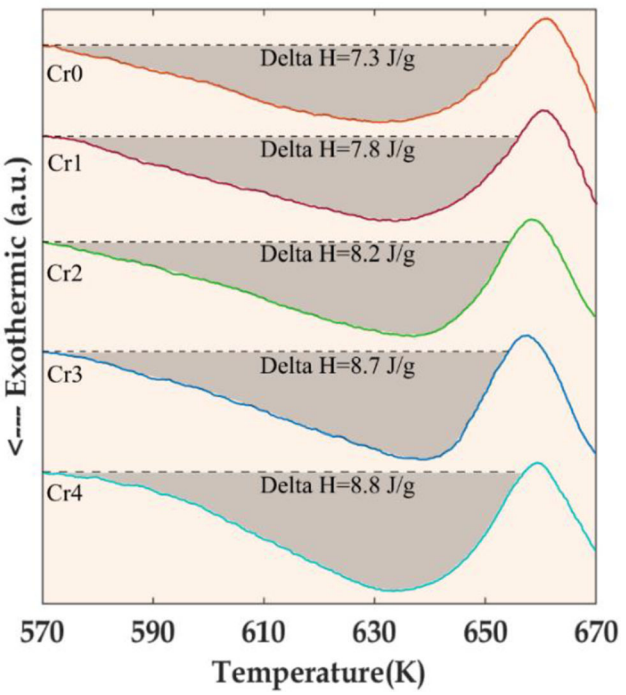

Fig. 3 Magnified relaxation regions of samples in DSC curves

The thermoplastic behavior of BMGs as a function of temperature can show the crystallization behavior. Therefore, the viscosity characteristics of BMG samples in the range of super-cooled liquid region were analyzed to better understand the crystallization evolution. The change in the height of samples under a constant load during the temperature increase is related to the viscosity parameter [44]:

$$\eta = -2hF^3\left[3\pi a^4\left(\frac{\mathrm{d}h}{\mathrm{d}t}\right)\right]^{-1} \quad (5)$$

In which a and h are the radius and height of samples, respectively, and F introduces the applied load. Figure 4 demonstrates the viscosity parameter as a function of temperature in all the samples. At the beginning of curves, the viscosity of samples gradually declines with the increase in temperature; however, it quickens at the super-cooled liquid region. This indicates that the elevated temperature accelerates the cooperative atomic movement under a certain external load. Moreover, it is observed that the Cr addition leads to the different behaviors in the super-cooled liquid region. The peaks in this region confirm the crystallization events, which is also presented in DSC curves. For the Cr-free sample, the second peak, i.e., high temperature one, is sharper which indicates the domination of high temperature crystallization in the system. With the increase in Cr content up to 3%, a reverse trend occurs and the first peak tends to become bigger so that for the sample with 3% Cr, the first peak dominates in the system. It is also worth mentioning that the Cr addition widens the region of viscosity at the peak's position in the curves. It means that a wide range of temperature at super-cooled liquid region is provided for crystallization. In another words, the crystallization in Cr-content samples is accompanied with a gradual evolution. This event is due to the fact that the Cr-content BMGs have a wide range of potential energy

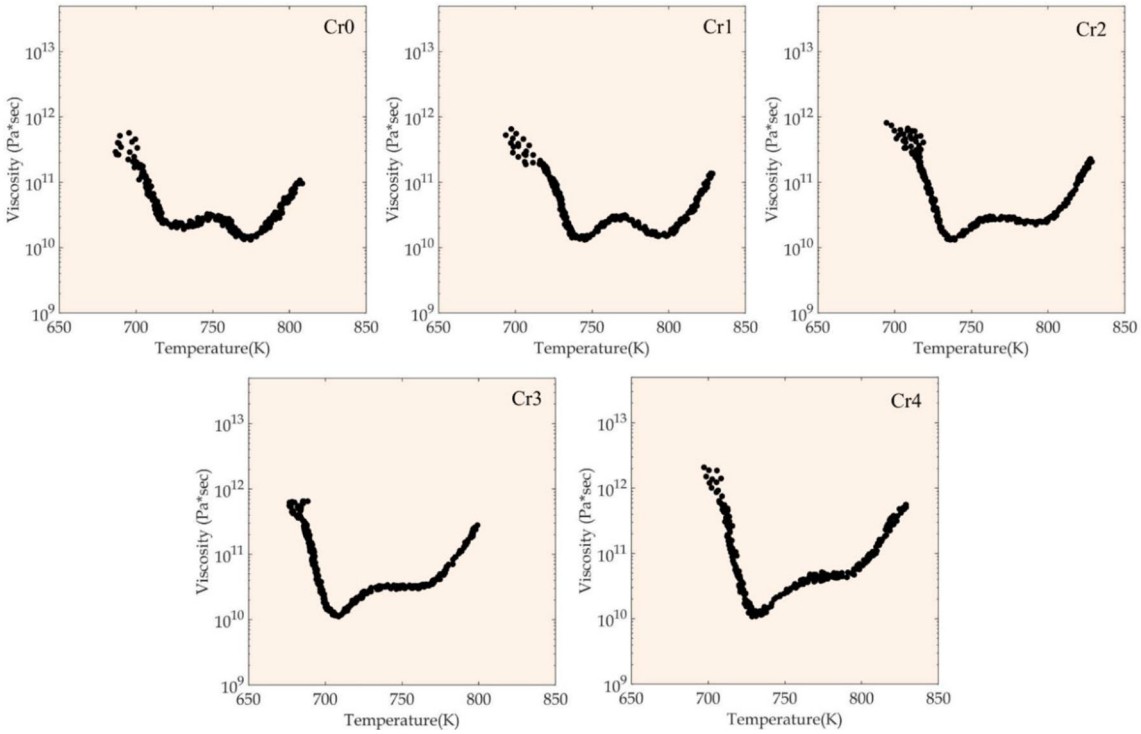

Fig. 4 Viscosity evolution in the super-cooled liquid region of samples

levels in their structure and therefore the crystallization would happen in broad temperature range at the mentioned region.

Extracted from nanoindentation test, the load–displacement curves of BMGs are given in Fig. 5a. It can be seen that the pop-in events increase with the rise in Cr content; however, their size becomes smaller. The pop-in events are closely related to the local deformation, i.e., shear bands, in the glassy alloy [45]. Our results indicate that the minor addition of Cr may induce multiple shear bands in the material and improve the homogenous plasticity under the loading, while the Cr-free sample suffers from the main big shear events embedding the majority of induced strain in local sites [46]. This result is due to the structural heterogeneity caused by the Cr microalloying in the BMG structure. The more the structural heterogeneity is the finer shear band formation is achieved. The hardness and Young modulus calculations also justify that the minor addition of Cr improves plasticity; however, it comes at the expense of strength (see Fig. 5b). Finally, it is summarized that the optimized Cr microalloying process induces the disordering event in the atomic structure, enhances the enthalpy of structural relaxation, changes the crystallization evolution in the super-cooled liquid region and improves the plasticity of Zr-based BMG.

4 Conclusion

In this work, the effects of Cr microalloying on the inherent features of ZrCoAlCr were studied and discussed in details. According to the results, minor addition of Cr led to the decrement of SRO and MRO structures in the glassy material and the increase in free volumes and nanoscale disordered configurations. Moreover, the crystallization event in the BMG was changed by Cr addition so that the trace element intensified the low temperature peak in DSC curves. The results also implied that the micromechanical properties of BMG improved with the increase in Cr content so that the number of serrations on the load–displacement curve increased, which indicated the enhancement of shear band population under the loading.

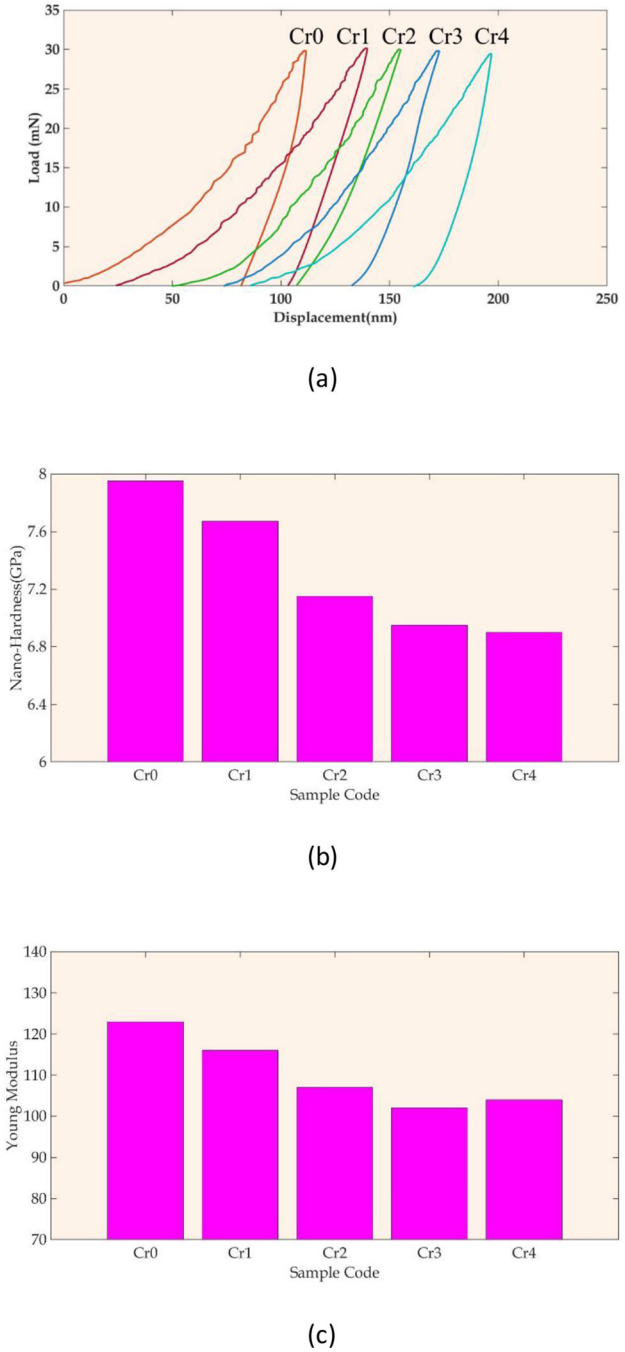

Fig. 5 **a** Load–displacement curves from nanoindentation results. **b** Nanohardness values and **c** Young's modulus for all the samples

References

[1] M M Khan, A Nemati, Z U Rahman, U H Shah, H Asgar, and W Haider, *Crit. Rev. Solid State Mater. Sci.* **43** (2018) 233.

[2] V T Nguyen, T H Li, S M Song, Y C Liao, P H Tsai, P C Wong, V C Nguyen, and J S C Jang, *Mater. Lett.* **256** (2019) 126650.

[3] N Dancholvichit, S G Kapoor, and S M Salapaka, *J. Manuf. Process.* (2020).

[4] G Praveen Kumar, M Jafary-Zadeh, R Tavakoli, and F Cui, *J. Biomed. Mater. Res. Part B Appl. Biomater.* **105** (2017) 1874.

[5] N T Panagiotopoulos, K Georgarakis, A M Jorge Jr, M Aljerf, W J Botta, A L Greer, and A. R. Yavari, *Mater. Des*, **192** (2020) 108770.

[6] J Schroers, *Adv. Mater.* **22** (2010) 1566.

[7] N Li, W Chen, and L Liu, *JOM* **68** (2016) 1246.

[8] M T Asadi Khanouki, R Tavakoli, and H Aashuri, *J. Alloys Compd.* **770** (2019) 535.

[9] M C Li, M Q Jiang, G Li, L He, J Sun, and F Jiang, *Intermetallics77* (2016) 34.

[10] J.-L. Gu, Y. Shao, and K.-F. Yao, *Materialia* **8** (2019) 100433.

[11] H Shi, C Tang, X Zhao, Y Ding, L Ma, and X Shen, *J. Non. Cryst. Solids* **537** (2020) 120013.

[12] J C Qiao, B A Sun, J Gu, M Song, J-M Pelletier, J W Qiao, Y Yao, and Y Yang, *J. Alloys Compd.* **724** (2017) 921.

[13] S Lin, Z Zhu, S Ge, L Zhang, D Liu, Y Zhuang, H Fu, H Li, A Wang, and H Zhang, *J. Mater. Sci. Technol.* **50** (2020) 128.

[14] S Hasani, P Rezaei-Shahreza, A Seifoddini, and M Hakimi, *J. Non. Cryst. Solids* **497** (2018) 40.

[15] R Hubek, M Seleznev, I Binkowski, M Peterlechner, S V Divinski, and G Wilde, *J. Appl. Phys.* **124** (2018) 225103.

[16] N Hua and W Chen, *J. Alloys Compd.* **693** (2017) 816.

[17] D Liang, X Wei, C Chang, J Li, X Wang, and J Shen, *J. Alloys Compd.* **731** (2018) 1146.

[18] D Cao, Y Wu, X J Liu, H Wang, X Z Wang, and Z P Lu, *J. Alloys Compd.* **777** (2019) 382.

[19] W Zai, H C Man, Y Su, G Li, and J Lian, *Mater. Chem. Phys.* (2020) 123555.

[20] S Bera, P Ramasamy, D Şopu, B Sarac, J Zálešák, C Gammer, M Stoica, M Calin, and J Eckert, *J. Alloys Compd.* **793** (2019) 552.

[21] J Wu, Z Zhou, J Yi, and Z Peng, *J. Therm. Anal. Calorim.* (2020).

[22] M Samavatian, R Gholamipour, V Samavatian, and F Farahani, *Mater. Res. Express* **6** (2019) 65202.

[23] Z S Jin, Y. J. Yang, Z. P. Zhang, X. Z. Ma, J. W. Lv, F. L. Wang, M. Z. Ma, X. Y. Zhang, and R. P. Liu, *J. Alloys Compd. 806* (2019) 668.

[24] A H Cai, J Tan, D W Ding, H Wang, Y Liu, H Wu, Q An, H Ning, and G J Zhou, *Mater. Chem. Phys.* **251**,(2020) 123072.

[25] M Malekan, R Rashidi, and S G Shabestari, *Vacuum* **174** (2020) 109223.

[26] F Hu, C Yuan, Q Luo, W Yang, and B Shen, *J. Non. Cryst. Solids* **525** (2019) 119681.

[27] X Niu, G Yao, J Qiao, S Feng, and S Pan, *Comput. Mater. Sci.* **171** (2020) 109285.

[28] A Mizuno, T Harada, and M Watanabe, *Phys. Status Solidi* (2020) 2000140.

[29] W H Wang, *Prog. Mater. Sci.* **52** (2007) 540.

[30] Y Chen, C Tang, K Laws, Q Zhu, and M Ferry, *J. Alloys Compd.* **820** (2020) 153079.

[31] J Huo, J-Q Wang, and W-H Wang, *J. Alloys Compd.* **776** (2019) 202.

[32] M Mohammadi Rahvard, M Tamizifar, and S M A Boutorabi, *J. Therm. Anal. Calorim.* **134** (2018) 903.

[33] M Mohammadi Rahvard, M Tamizifar, and S M A Boutorabi, *J. Non. Cryst. Solids* **491** (2018) 114.

[34] J Zhu, C. Wang, J. Han, S. Yang, G. Xie, H Jiang, and X Liu, *Intermetallics* **92** (2018) 55.

[35] A Sharma, P Singh, D D Johnson, P K Liaw, and G Balasubramanian, *Sci. Rep.* **6** (2016) 31028.

[36] C Chattopadhyay and B S Murty, *Scr. Mater.* **116** (2016) 7.

[37] Y. Du, W. Han, Q. Zhou, Y. Xu, H. Zhai, V. Bhardwaj, and H Wang, *Materialia*, **9** (2020) 100561.

[38] J C Qiao, J Cong, Q Wang, J M Pelletier, and Y Yao, *J. Alloys Compd.* **749** (2018) 262.

[39] M Zhou, J Zhou, J Wei, M Yang, and L Ma, *J. Non. Cryst. Solids* **455**, (2017) 1.
[40] Y Du, W Han, Q Zhou, Y Xu, H Zhai, V Bhardwaj, and H Wang, *J. Alloys Compd.* **835** (2020) 155247.
[41] Z Pan and T J Rupert, *Comput. Mater. Sci.* **131** (2017) 62.
[42] X F Zhang, S P Pan, J W Qiao, and A D Lan, *Comput. Mater. Sci.* **128** (2017) 343.
[43] M Samavatian, R Gholamipour, A A Amadeh, and S Mirdamadi, *J. Non. Cryst. Solids* **506** (2019) 39.
[44] J Zhu, M Yang, C Wang, S Yang, J Han, G Xie, and X Liu, *J. Alloys Compd.* **781** (2019) 8.
[45] C C Yuan, Z W Lv, C M Pang, W W Zhu, X-L Wang, and B L Shen, *J. Alloys Compd.* **806** (2019) 246.
[46] D Şopu, S Scudino, X L Bian, C Gammer, and J Eckert, *Scr. Mater.* **178** (2020) 57.